Cyclooxygenase-2 regulates mesenchymal cell differentiation into the osteoblast lineage and is critically involved in bone repair

Online first publication

Xinping Zhang,[1] Edward M. Schwarz,[1] Donald A. Young,[2] J. Edward Puzas,[1] Randy N. Rosier,[1] and Regis J. O'Keefe[1]

[1]The Center for Musculoskeletal Research, University of Rochester Medical Center, and
[2]Department of Medicine/Endocrinology, University of Rochester School of Medicine and Dentistry, Rochester, New York, USA

Address correspondence to: Regis J. O'Keefe, The Center for Musculoskeletal Research, University of Rochester Medical Center, 601 Elmwood Avenue, Rochester, New York 14642, USA.
Phone: (716) 273-4255; Fax: (716) 442-3214; E-mail: Regis_OKeefe@URMC.rochester.edu.

Preclinical and clinical studies suggest a possible role for cyclooxygenases in bone repair and create concerns about the use of nonsteroidal antiinflammatory drugs in patients with skeletal injury. We utilized wild-type, *COX-1*$^{-/-}$, and *COX-2*$^{-/-}$ mice to demonstrate that COX-2 plays an essential role in both endochondral and intramembranous bone formation during skeletal repair. The healing of stabilized tibia fractures was significantly delayed in *COX-2*$^{-/-}$ mice compared with *COX-1*$^{-/-}$ and wild-type controls. The histology was characterized by a persistence of undifferentiated mesenchyme and a marked reduction in osteoblastogenesis that resulted in a high incidence of fibrous nonunion in the *COX-2*$^{-/-}$ mice. Similarly, intramembranous bone formation on the calvaria was reduced 60% in *COX-2*$^{-/-}$ mice following in vivo injection of FGF-1 compared with either *COX-1*$^{-/-}$ or wild-type mice. To elucidate the mechanism involved in reduced bone formation, osteoblastogenesis was studied in bone marrow stromal cell cultures obtained from *COX-2*$^{-/-}$ and wild-type mice. Bone nodule formation was reduced 50% in *COX-2*$^{-/-}$ mice. The defect in osteogenesis was completely rescued by addition of prostaglandin E2 (PGE_2) to the cultures. In the presence of bone morphogenetic protein (BMP-2), bone nodule formation was enhanced to a similar level above that observed with PGE_2 alone in both control and *COX-2*$^{-/-}$ cultures, indicating that BMPs complement COX-2 deficiency and are downstream of prostaglandins. Furthermore, we found that the defect in *COX-2*$^{-/-}$ cultures correlated with significantly reduced levels of *cbfa1* and *osterix*, two genes necessary for bone formation. Addition of PGE_2 rescued this defect, while BMP-2 enhanced *cbfa1* and *osterix* in both *COX-2*$^{-/-}$ and wild-type cultures. Finally, the effects of these agents were additive, indicating that COX-2 is involved in maximal induction of osteogenesis. These results provide a model whereby COX-2 regulates the induction of *cbfa1* and *osterix* to mediate normal skeletal repair.

J. Clin. Invest. **109**:1405–1415 (2002). doi:10.1172/JCI200215681.

Introduction

Prostaglandins have been shown to play an important role in bone metabolism (1, 2). The rate-limiting step in prostaglandin production is controlled by the cyclooxygenases COX-1 and COX-2. The current paradigm to explain the role of these enzymes is that COX-1 is constitutively produced and functions to maintain homeostasis, whereas COX-2 acts as a stress response gene and is responsible for high levels of prostaglandin production during inflammation (3). The relative roles of these enzymes in bone remodeling have been recently resolved in studies with mice genetically deficient for COX-1 or COX-2. Mice lacking COX-2 but not COX-1 expression display reduced bone resorption in response to parathyroid hormone (PTH) or 1,25-hydroxyl vitamin D_3 (4). Previously, we also demonstrated that COX-2 is required for wear debris–induced osteoclastogenesis and osteolysis in an in vivo mouse calvaria model (5).

In addition to bone resorption, COX-2 may also have a role in bone formation. Systemic or local injection of PGE_2 stimulates bone formation (6, 7). Increased lamellar bone formation in response to mechanical strain is mediated by COX-2 (8, 9). Although both COX-1 and COX-2 have been identified in osteoblasts, the differential roles of the two cyclooxygenases in bone formation remain unclear. The use of COX-1 (10, 11) and COX-2 (10, 11) knockout animals makes it possible to assess the role of these enzymes in regulating bone cell function and the response to local and systemic factors. In particular, *COX-2*$^{-/-}$ mice have decreased bone density compared with normal littermates (12).

Genetic knockout studies have also identified genes that are specifically required for osteoblast differenti-

ation and bone formation. Two of these genes are *cbfa1* and *osterix*. Cbfa1 is a member of the RUNX family of transcription factors and is involved in the regulation of several osteoblast-specific genes, including osteocalcin (13, 14). The tissue expression pattern of *cbfa1* is highly restricted, and its importance in bone is apparent from the phenotype of the *cbfa1*$^{-/-}$ mouse, which lacks osteoblasts (13, 14). Osterix is a helix-loop-helix transcription factor identified by subtraction hybridization in C2C12 cells stimulated to undergo differentiation following treatment with BMP-2 (15). The *osterix*$^{-/-}$ mouse also lacks osteoblasts and is characterized by the persistence of undifferentiated mesenchyme (15). However, mice lacking *osterix* have undifferentiated mesenchymal cells expressing *cbfa1* and thus have committed to the osteoblast lineage. Thus, while both *cbfa-1* and *osterix* are necessary for mesenchymal cell differentiation to osteoblasts, *osterix* acts downstream of *cbfa1*.

The metabolites of cyclooxygenase activity have long been suspected to have a role in skeletal reparative processes. The levels of prostaglandins E and F are increased between days 3 and 14 in tissues obtained from rabbit tibia fractures (16). Multiple nonsteroidal antiinflammatory drugs (NSAIDs), whose primary targets are the cyclooxygenases, have been reported to inhibit fracture healing in animal studies (17, 18). A recent clinical study showed a marked association between nonunion of the femoral shaft and the use of NSAIDs (19). Human studies further demonstrate a significant reduction in the rate of spinal fusion in patients taking NSAIDs (20). In contrast, the administration of PGE_2 has increased the rate of fracture healing in several animal models (21–23), indicating that the metabolites of cyclooxygenase may be necessary for efficient bone healing.

Fracture healing is a complex process that requires the recruitment, proliferation, and differentiation of mesenchymal stem cells into chondrocytes and osteoblasts and involves both endochondral ossification, whereby bone formation occurs through a cartilage intermediate, and intramembranous ossification, in which bone forms directly from differentiated osteoblasts (24, 25). Healing occurs when the bone gap is bridged by woven bone and is completed with remodeling and the formation of mature lamellar bone. The relative role of COX-1 and COX-2 isoforms, and the target cells and tissues involved in adult bone repair, have not been clearly defined. The elucidation of the roles of COX-1 and COX-2 in bone healing is of paramount importance given the widespread clinical use of cyclooxygenase inhibitors.

In this study, we used three in vivo experimental models to examine the bone healing in wild-type mice and mice genetically deficient for each enzyme (*COX-1*$^{-/-}$ and *COX-2*$^{-/-}$). We demonstrate that COX-2 is required for both intramembranous and endochondral bone formation during bone repair, while COX-1 does not have a critical role in these processes. Furthermore, we establish that *cbfa-1* and *osterix* are regulated by COX-2, and that decreased expression of these genes may contribute to defective bone repair in *COX-2*$^{-/-}$ mice.

Methods

Experimental animals. All animal studies were conducted in accordance with principles and procedures approved by the University of Rochester Institutional Review Board. Male and female mice, 6–8 weeks old, were used in the experiments. *COX-1*$^{-/-}$ and *COX-2*$^{-/-}$ mice (10, 11) were originally obtained from the breeding colony at the University of North Carolina (Chapel Hill, North Carolina, USA). They were of hybrid C57BL/6J × 129/ola genetic background, intercrossed for about 30 generations. Mice were genotyped using PCR as described (26). Littermate controls are used in all the studies.

Fracture healing model. Mice were anesthetized with ketamine and xylazine intraperitoneally. The skin was incised overlying the left knee. A 0.25-mm metal pin

Figure 1
Fracture healing is delayed in *COX-2*$^{-/-}$ mice. Diaphyseal fractures were created in 2- to 3-month-old wild-type, *COX-1*$^{-/-}$, and *COX-2*$^{-/-}$ mice as described in Methods. Representative radiographs of wild-type (**a**, **d**, and **g**), *COX-1*$^{-/-}$ (**b**, **e**, and **h**), and *COX-2*$^{-/-}$ (**c**, **f**, and **i**) mice obtained on days 7 (**a**–**c**), 14 (**d**–**f**), and 21 (**g**–**i**) after fracture are shown. Of note is the absence of fracture callus and bony union in the *COX-2*$^{-/-}$ mice.

Table 1
Radiographic assessments of fracture healing in wild-type, *COX-1*$^{-/-}$, and *COX-2*$^{-/-}$ mice.

	Day 14		Day 21	
	Callus	Union	Callus	Union
Wild-type	14/15	4/15	10/10	8/10
COX-2$^{-/-}$	5/14^{A}	0/14^{B}	7/8	3/8^{B}
COX-1$^{-/-}$	5/6	0/6	6/6	5/6

Radiographs of wild-type, *COX-1*$^{-/-}$, and *COX-2*$^{-/-}$ mice obtained on days 7, 14, and 21 after fracture were evaluated for the presence of mineralized callus and bony union by three blinded observers. The data are presented as the number of mice with positive findings divided by the total number of mice in the group. Binomial *z* distribution was used to determine the statistical differences between the *COX-2*$^{-/-}$ mice and wild-type mice ($^{A}P < 0.01$, $^{B}P < 0.05$). No significant differences between *COX-1*$^{-/-}$ mice and wild-type mice were found.

was inserted through the patellar tendon into the medullary canal of the tibia as previously described (27). The incision was closed and a mid-diaphyseal fracture was created using three-point bending with an Einhorn device using a standardized force (28, 29). Immediately after tibia fracture, 0.5 mg/kg Buprenorphine (Abbott Labs, North Chicago, Illinois, USA) was administered subcutaneously to each mouse with repeated injections every 12 hours for 3 days for pain control. Radiographs were obtained at 7, 14, and 21 days under anesthesia using a Faxitron x-ray system (Faxitron X-ray, Wheeling, Illinois, USA). The healing was monitored radiographically weekly using x-rays that were blindly scored by three orthopedic surgeons for the presence of calcified fracture callus and evidence of bone union. Mice were sacrificed on day 7, 14, and 21 by cervical dislocation. Tibias were harvested, fixed in 10% formalin, and embedded in paraffin. Sections were stained as described previously (30). Briefly, the slides were dipped in 1% acid alcohol (1% HCl made in 70% ethyl alcohol) for 30 seconds, then stained in Alcian blue/hematoxylin solution (0.5% hematoxylin, 5% aluminum ammonium sulfate, 0.05% sodium iodate, 0.5% Alcian blue, 50% glycerol, 0.02% glacial acetic acid) for 30 minutes at room temperature. The slides were washed with distilled water and then dipped in 1% acid alcohol for 2–3 seconds. Slides were washed again in distilled water and then treated in 0.5% ammonium water for 15 seconds, followed by another wash with water and treatment in 95% alcohol for 1 minute. After the stain with Alcian blue and hematoxylin, eosin–orange G (1.2% eosin in 90% alcohol plus 1% phloxine B and 2% orange G) was used to counterstain the slides for 1 minute 30 seconds. The slides were then dipped in 3 containers containing 95% alcohol and were left in the third container for 3 minutes, followed by mounting with Permount (VWR Scientific, South Plainfield, New Jersey, USA).

Mouse calvarial postinflammatory bone formation model. Eight-week-old female mice were anesthetized by peritoneal injection of 80 mg/kg of ketamine and 5–7 mg/kg of xylazine. A 1-cm midline sagittal incision was made above the calvaria. Titanium (Ti; 30 mg) particles were placed evenly on top of the calvarial bones, leaving the periosteum intact. After implantation, the skin was closed with 4-0 Ethilon suture. At day 10, mice were sacrificed by cervical dislocation and calvaria were removed, fixed in 10% formalin, decalcified in 10% EDTA, dehydrated in graded alcohols, and embedded in paraffin. Representative sections were cut and stained with hematoxylin and eosin (H&E), as described previously (31). For these experiments, we assessed bone formation on the calvarial surface in the lateral aspect of the parietal bone where bone resorption is minimal. Six sections spanning a total of 600 μm were obtained from each calvaria, and the width of new bone was quantified from the section with maximal bone formation. Newly synthesized bone is identified in the decalcified calvarial sections by its differential staining with eosin as well as by the woven structure of the collagen when viewed under polarized light. The mean percentage of periosteal new bone area compared with the total calvaria bone was quantified with histomorphometry.

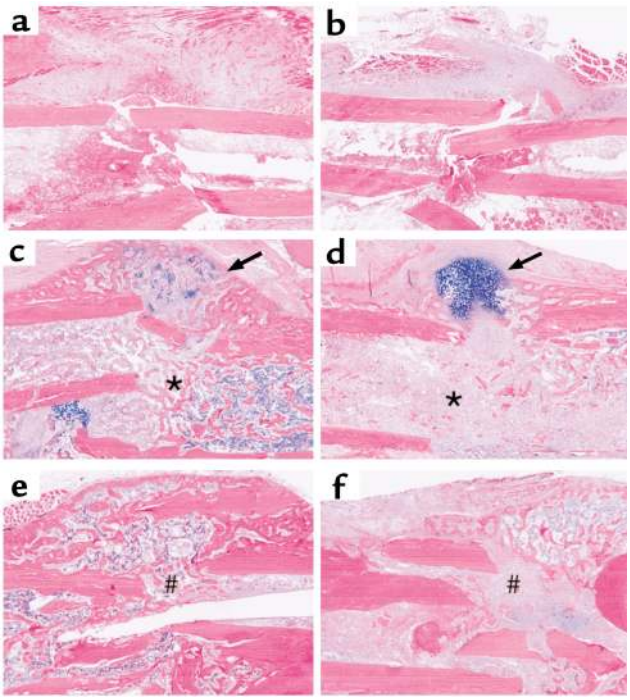

Figure 2
Histologic evidence of defective fracture healing in *COX-2*$^{-/-}$ mice. Histologic sections were obtained from tibial fractures of adult wild-type (**a**, **c**, and **e**) and *COX-2*$^{-/-}$ mice (**b**, **d**, and **f**) at 7 (**a** and **b**), 14, (**c** and **d**), and 21 days (**e** and **f**) after fracture, and stained with Alcian blue/hematoxylin as described in Methods. Fractures in wild-type mice undergo extensive calcification resulting in little residual cartilage (arrow) and extensive woven bone formation (asterisk) by day 14 (**c**). This progresses to a remodeling bony union (#) by day 21. In the *COX-2*$^{-/-}$ mice there is little evidence of endochondral bone formation in the medullary canal, which is filled with undifferentiated mesenchymal tissue (asterisk) on day 14 (**d**). Concurrently, significant amounts of unmineralized cartilage persists (arrow) (**d**). By 21 days there are large amounts of fibrotic tissue (#) between the fractured bones, evidence of a fracture nonunion (**f**).

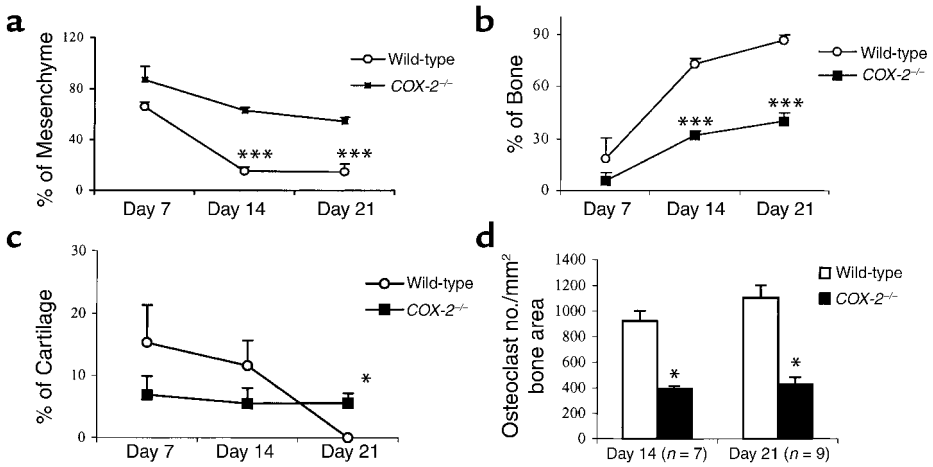

Figure 3
Quantitative analysis of fracture callus in wild-type and *COX-2*$^{-/-}$ mice at 7, 14, and 21 days after fracture. Tissue sections from wild-type and *COX-2*$^{-/-}$ mice harvested on days 7 (n = 5), 14 (n = 7), and 21 (n = 9) after fracture were stained with Alcian blue/hematoxylin or for tartrate resistant acid phosphate (TRAP) as described in Methods. All slides were analyzed using Osteometrics software, (Osteometrics Inc., Atlanta, Georgia, USA) and percentages of mesenchymal tissue (**a**), bone (**b**), and cartilage (**c**) relative to the total fracture area are presented as the mean ± SEM. (**d**) Osteoclast numbers (TRAP-positive cells) per mm^2 bone area were quantified as described in Methods and are presented as the mean ± SEM. Student's t test was used to determine the statistical differences between each group. *P < 0.05, ***P < 0.001.

Local FGF injection. Recombinant human FGF-1 was obtained from Rhone-Poulenc Rorer (Vitry, France). Local injections were made subcutaneously over both sides of the mouse calvaria. They were injected four times a day for 3 days in 10 μl vehicle containing 0.1% BSA in PBS (pH 7.4). The dose of FGF-1 used was 1 μg/day/mouse based upon prior studies (32). Mice were euthanized by CO_2 14 days after the initial injection. Mouse calvaria were harvested and processed. The samples were embedded in paraffin, and 4-μm cross sections were cut parallel to the coronary suture. At least six sections 150 μm apart were cut for each mouse calvaria. Sections were stained with orange G method as previously described (30). Newly synthesized bone is identified in the decalcified calvarial sections by its differential staining with eosin as well as by the woven structure of the collagen when viewed under polarized light. The mean percentage of periosteal new bone area compared with the total calvaria bone was quantified with histomorphometry (31).

In situ hybridization. ^{35}S-UTP-labeled sense and antisense riboprobes were synthesized from plasmids (kindly provided by Jill Helms, University of California, San Francisco, USA) with insertions of mouse

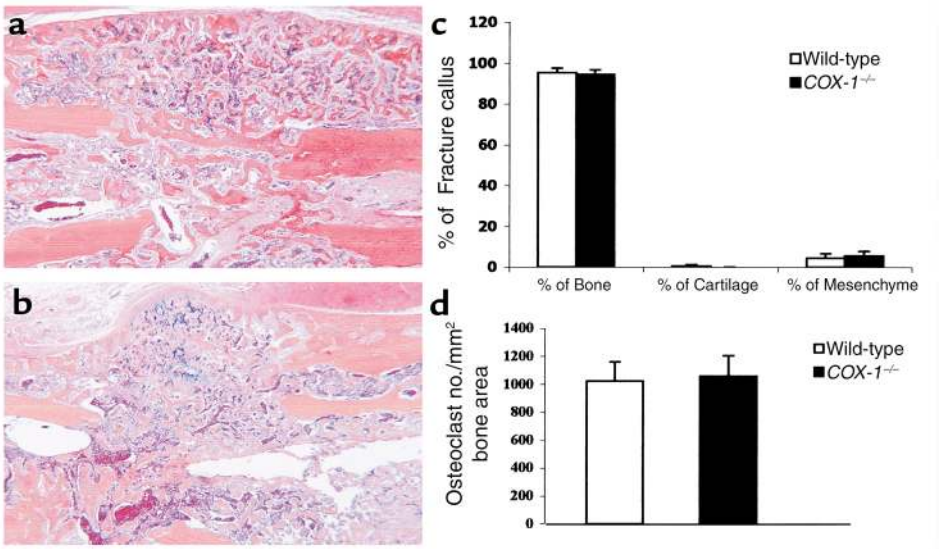

Figure 4
Normal fracture healing in *COX-1*$^{-/-}$ mice. Histologic sections were obtained from tibial fractures of adult wild-type (**a**) and *COX-1*$^{-/-}$ (**b**) mice (n = 5) on day 21 after fracture and stained with Alcian blue/hematoxylin as described in Methods. Quantification of the tissue compositions (**c**) and osteoclast numbers (**d**) are presented as described in Figure 3. No significant differences were observed.

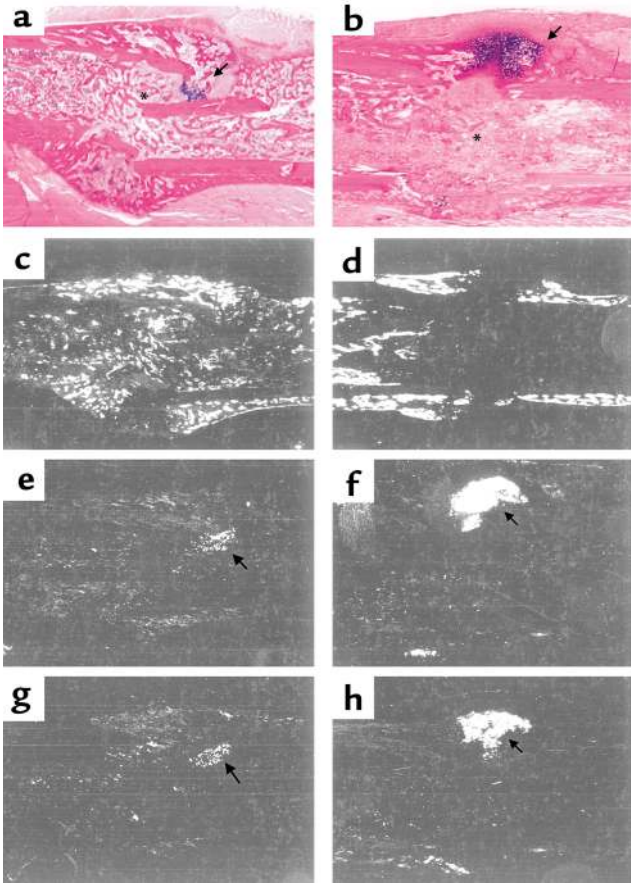

Figure 5
Characterization of defective fracture healing in *COX-2*$^{-/-}$ mice by in situ hybridization. Histologic sections of the fracture callus of wild-type (**a**, **c**, **e**, and **g**) and *COX-2*$^{-/-}$ mice (**b**, **d**, **f**, and **h**), 14 days after fracture, were stained with Alcian blue/hematoxylin (**a** and **b**). Serial sections were used for in situ hybridization with probes specific for *osteocalcin* (**c** and **d**), *col2* (**e** and **f**), and *colX* (**g** and **h**). The gene expression profile confirms the persistence of cartilage (arrows) and the decrease in osteogenesis (asterisks) in *COX-2*$^{-/-}$ mice.

osteocalcin, *type II collagen* (*col2*), and *type X collagen* (*colX*) as previously described (27, 28). The specific activity of the probes was determined by radioactivity. The sections were incubated in hybridization buffer (50% formamide, 0.3 M NaCl, 20 mM Tris HCl, 5 mM EDTA, 10% dextran sulfate, 0.02% Ficoll, 0.02% BSA, 0.02% polyvinyl pyrrolidone, and 0.5 mg/ml yeast RNA) containing each riboprobe at 10,000 cpm/μl, and hybridization was performed at 55°C overnight. Nonspecifically bound probe was hydrolyzed with RNase A (20 μg/ul), and final washes were carried out at high stringency at 55°C with 2× SSC/50% formamide as described previously (28). Emulsion-dipped slides were exposed for about 7–14 days depending upon the intensity of the signals.

Bone marrow osteoblast differentiation assays. Bone marrow cells were isolated from 2- to 3-month-old mice as described previously (28). Mice were sacrificed by cervical dislocation. Femora and tibiae were removed aseptically and dissected free of adherent soft tissue. The bone ends were cut, and bone marrow cells were flushed from marrow cavity by slowly injecting MEM at one end of the bone using a sterile 21-gauge needle. The marrow suspension was dispersed gently by pipetting several times to obtain a single cell suspension. 0.5×10^6 to 5×10^6 bone marrow cells per 10 cm^2 were plated on 60-mm culture dishes or six-well plates and cultured in α-MEM containing 15% FBS (HyClone Laboratories, Logan, Utah, USA) for 5 days. The medium was removed by the end of the fifth day, and fresh MEM with 15% FBS, 50 μM of ascorbic acid, and 10 mM β-glycerophosphate were added. Cells were maintained for 21 days with medium changes for every 5 days. On day 0, 10^{-7} M PGE_2 (Cayman Chemical, Ann Arbor, Michigan, USA) was added, and 200 ng/ml of recombinant murine BMP-2 (a gift from Genetics Institute Inc., Cambridge, Massachusetts, USA) was added on the fifth day. Fresh factors at the same indicated concentration were added with medium change every 5 days.

Real time PCR assays. To examine the gene expression, cells were cultured for 10–14 days and total RNA was extracted using RNeasy kit (QIAGEN Inc., Valencia, California, USA). Single-stranded cDNA was made using a reverse transcription kit from CLONTECH Laboratories Inc. (Palo Alto, California, USA). PCR was performed on Rotor-Gene 2000 real-time amplification operator (Corbett Research, Mortlake, Australia). The primers for *osteocalcin*, *cbfa1*, *BMP-2*, *actin*, and *osterix* were from Invitrogen Corp. (San Diego, California, USA). The oligonucleotide primers used in the study are the following: *cbfa1* forward, 5′-GCCACACTTTCCACACTCTC-3′; *cbfa1* reverse, 5′-CACTTCTGCTTCTTCGTTCTC-3′; *osterix* forward, 5′-TGAGGAAGAAGCCCATTCAC-3′; *osterix* reverse, 5′-ACTTCTTCTCCCGGGTGTG-3′; *actin* forward, 5′-AGATGTGGATCAGCAAGCAG-3′; *actin* reverse, 5′-GCGCAAGTTAGGTTTTGTCA-3′. The PCR reactions contained a final concentration of 1× SYBR Green PCR Master Mix (Applied Biosystems, Warrington, United Kingdom), 10 μM specific primers, and 2.5 ng of cDNA. The relative levels of mRNA of a specific gene were calculated using the standard curve generated from cDNA dilutions. The mean cycle threshold (Ct) values from quadruplicate measurements were used to calculate the gene expression, with normalization to *actin* as an internal control. Calculations of the relative level of gene expression were conducted according to the instructions from User's Bulletin (P/N 4303859) from Applied Biosystems.

Statistical analysis. Data are expressed as means ± SEM. Statistical significance was determined by Student's *t* test. A *P* value of less than 0.05 was considered statistically significant. To compare the incidence of callus formation and unions of the fractures between different groups of animals, the binomial *z* distributions were used and a *P* value of less than 0.05 was considered

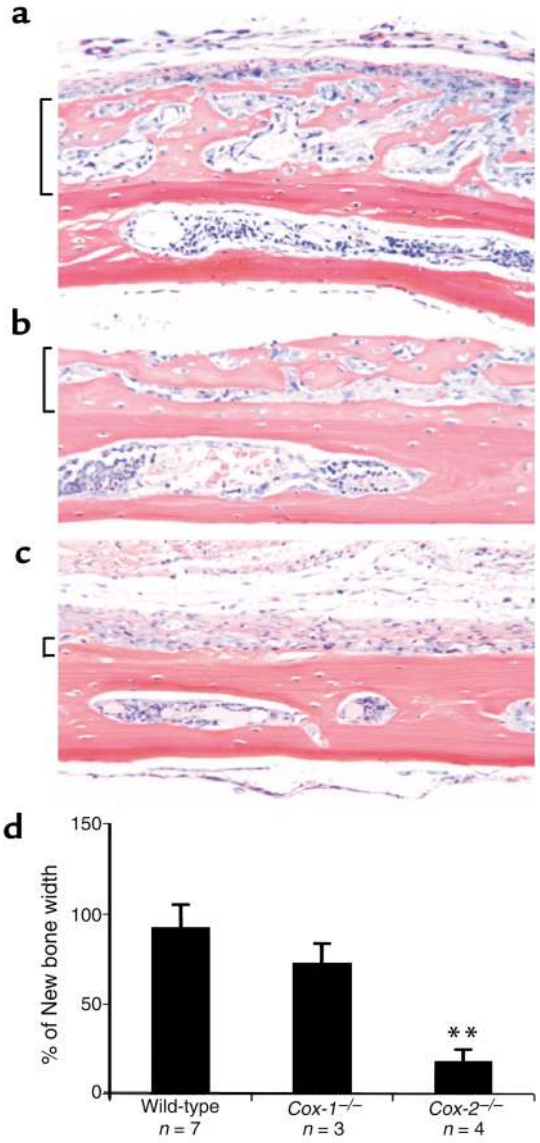

Figure 6
Inflammation-induced intramembranous bone formation is reduced in *COX-2*$^{-/-}$ mice. Titanium particles were surgically implanted onto the calvaria of wild-type (**a**), *COX-1*$^{-/-}$ (**b**), and *COX-2*$^{-/-}$ (**c**) mice as described in Methods, and representative H&E-stained sections are shown. Ectopic bone formation was measured, and the percentage of new bone width (brackets) is presented as the mean ± SEM (**d**). Statistical significance compared with wild-type is indicated (**$P < 0.01$).

statistically significant. For real-time PCR analysis, statistical analyses were conducted according to the instructions from Applied Biosystems. Student's *t* test was used to examine the statistical significance.

Results

A critical role of COX-2 in fracture repair. To determine whether cyclooxygenase isoforms are involved in fracture healing, diaphyseal tibia fractures were created in 2- to 3-month-old wild-type, *COX-1*$^{-/-}$, and *COX-2*$^{-/-}$ mice using an established model (28, 29). Radiographs were taken at 7, 14, and 21 days (Figure 1) and independently and blindly reviewed by three orthopedic surgeons who determined the presence or absence of callus formation and bone union (Table 1). Calcified callus was apparent 14 days after fracture in 14 of 15 wild-type mice, compared with only 5 of 14 *COX-2*$^{-/-}$ mice ($P < 0.01$). By day 21, eight of ten wild-type animals had radiographic evidence of bone union compared with only three of eight *COX-2*$^{-/-}$ mice ($P < 0.01$). In these studies no significant differences were observed between *COX-1*$^{-/-}$ mice and their wild-type littermates at day 14 and day 21 after fracture.

Histologic features of fracture healing were examined in tissue sections obtained from mice 7, 14, and 21 days after fracture. Sections were stained with alcian blue and hematoxylin to distinguish cartilage, newly formed woven bone, and lamellar bone and confirmed a specific defect in fracture healing in *COX-2*$^{-/-}$ mice (Figures 2 and 3). By 7 days after fracture, the callus is characterized by mesenchymal cell proliferation and the initiation of chondrogenesis, which is similar in *COX-2*$^{-/-}$ and wild-type mice. At 14 days we observed several remarkable differences. In wild-type mice, abundant periosteal and intramedullary new bone formation has occurred and endochondral bone formation is being completed, with elimination of cartilage at the fracture junction. In contrast, we found a marked reduction of mesenchymal cell differentiation into cartilage or bone in the intramedullary bone cavity in *COX-2*$^{-/-}$ mice. Similarly, there was reduced periosteal bone formation and persistence of cartilage in the avascular zone at the junction of the fracture, with limited primary bone formation and remodeling characteristic of the final stages of endochondral bone formation. Quantitative histomorphometry demonstrated a significant increase in residual mesenchyme and an associated decrease in bone formation and osteoclast numbers in the *COX-2*$^{-/-}$ callus (Figure 3, a, b, and d). By 21 days, fracture healing is complete in wild-type animals, with evidence of bridging callus, disappearance of cartilage, and persistent remodeling of the callus. However, at this time, *COX-2*$^{-/-}$ fractures are characterized by persistence of mesenchyme, cartilage, and reduced bone formation with evidence of nonunion. Consistent with the radiographic findings, we were unable to detect any significant differences in fracture healing between wild-type and *COX-1*$^{-/-}$ mice using histologic methods (Figure 4).

In situ hybridization was performed on fracture callus at day 14 to examine the expression of markers of both cartilage and bone differentiation (Figure 5). Consistent with the histologic findings, there was a reduction in *osteocalcin* expression in *COX-2*$^{-/-}$ mice, with large areas of callus devoid of osteoblast differentiation. Expression of *col2* and *colX* was present in both *COX-2*$^{-/-}$ and wild-type calluses. Since *colX* is a marker of terminally differentiated cartilage, the findings suggest that the defect in bone formation is not due to a primary abnormality in the terminal differentiation of chondrocytes.

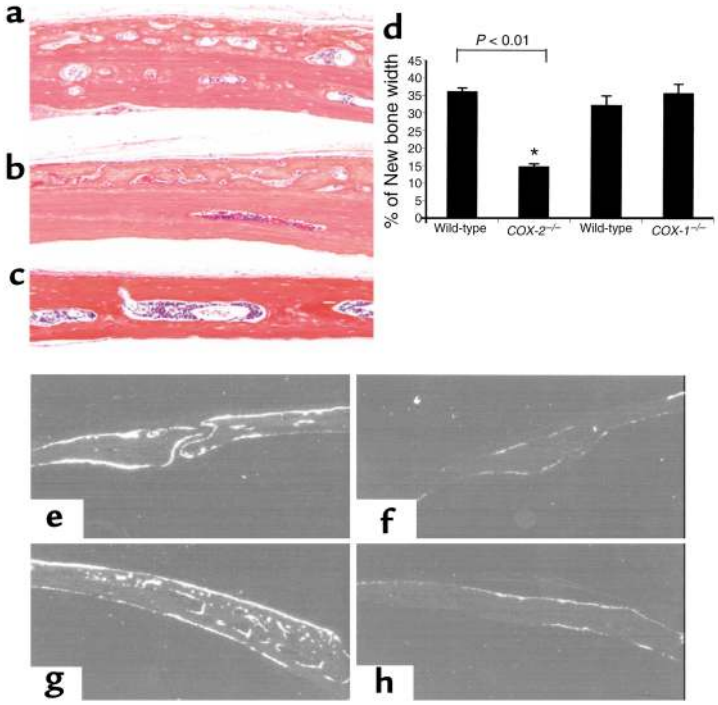

Figure 7
Defective intramembranous bone formation in *COX-2*$^{-/-}$ calvaria in response to FGF-1. FGF-1 was injected subcutaneously (1 μg/d for 3 days) on the calvaria of wild-type, *COX-1*$^{-/-}$, and *COX-2*$^{-/-}$ mice, and osteogenesis was analyzed by histomorphometry 14 days later as described in Methods. The photographs of representative H&E-stained sections from wild-type (**a**), *COX-1*$^{-/-}$ (**b**), and *COX-2*$^{-/-}$ mice (**c**) are shown at ×20 magnification. New bone width was measured at ×20 magnification, and the data from five animals in each group are presented as the mean ± SEM (**d**). Statistical significance compared with wild-type is indicated (*$P < 0.01$). Histology sections were examined by in situ hybridization using a riboprobe specific for *osteocalcin* as described in Methods. Dark-field photographs (**e**–**h**) were taken at ×4 magnification. The signal for *osteocalcin* mRNA was markedly reduced in *COX-2*$^{-/-}$ mice (**f** and **h**) compared with wild-type (**e** and **g**) at both the sagittal suture (**e** and **f**) and the lateral region (**g** and **h**) of the calvaria.

A critical role of COX-2 in intramembranous bone repair. Since the fracture healing studies suggest a primary defect in bone formation, we examined the role of COX-2 in two in vivo models of intramembranous bone formation that occur without a cartilage intermediate. In the first model, we examined reparative bone formation following inflammatory bone loss in response to titanium particles implanted onto the calvaria (33). Ten days after titanium implantation, robust intramembranous bone formation can be measured both on the resorbed endosteal surfaces in the marrow spaces, and on the unresorbed lateral periosteal surface of the parietal bones. We evaluated the role of cyclooxygenases in this model of intramembranous bone repair by quantifying the amount of new bone formed on the lateral periosteum in the wild-type, *COX-1*$^{-/-}$, and *COX-2*$^{-/-}$ mice. Previously we reported a significant decrease in the amount of bone formed on resorbed surfaces (5). Here we observed a 75% reduction in new bone formation on lateral periosteal surfaces adjacent to the region of bone resorption in *COX-2*$^{-/-}$ mice compared with wild-type and *COX-1*$^{-/-}$ mice (Figure 6).

In a second model devoid of inflammation and remodeling, we examined periosteal bone formation following the injection of FGF-1 (1 μg/d for 3 days) onto the calvarial surface of wild-type, *COX-1*$^{-/-}$, and *COX-2*$^{-/-}$ mice. Osteogenesis was analyzed by histomorphometry and in situ hybridization 14 days later. Periosteal bone formation was reduced by 67% in *COX-2*$^{-/-}$ mice compared with wild-type animals, while no defect was observed in periosteal bone formation in *COX-1*$^{-/-}$ mice (Figure 7, a–d). Consistent with this finding, in situ hybridization for *osteocalcin* gene expression revealed a marked decrease in the *COX-2*$^{-/-}$ calvaria compared with wild-type animals (Figure 7, e–h). These findings demonstrate the importance of COX-2 in intramembranous bone formation in response to diverse osteogenic signals.

Reduction of osteoblastic bone nodule formation in bone marrow stromal cells derived from COX-2$^{-/-}$ *mice*. In vitro studies were performed to evaluate the molecular mechanisms involved in the defective bone formation observed in *COX-2*$^{-/-}$ mice. In these experiments, bone marrow stromal cells were isolated from either *COX-1*$^{-/-}$ or *COX-2*$^{-/-}$ mice and their wild-type littermates and were stimulated to differentiate into osteoblasts in response to osteogenic signals. Osteoblastic bone nodule formation assays were performed in cultures maintained in medium containing 50 μM L-ascorbic acid and 10 mM β-glycerophosphate. After 21 days, Von Kossa staining revealed a 50% decrease in the number and area of mineralized bone nodules in the *COX-2*$^{-/-}$ cultures (Figure 8). In contrast, there was no difference observed in bone nodule formation between bone marrow cell cultures obtained from wild-type and *COX-1*$^{-/-}$ littermates (data not shown). Addition of PGE_2 (10^{-7} M) to the *COX-2*$^{-/-}$ cell cultures restored nodule formation to wild-type levels. To examine whether COX-2 is required for the induction of bone nodule formation by BMPs, 200 ng/ml BMP-2 was added to the cultures on day 5 and continued until day 21. We found that BMP-2 induced bone nodule formation in both wild-type and *COX-2*$^{-/-}$ cell cultures. The magnitude of the induction in nodule formation was similar, suggesting that BMPs are downstream of prostaglandins during osteoblastogenesis and bone formation. However, in cultures containing both exogenous PGE_2 and BMP-2, we observed an additional increase in nodule formation compared

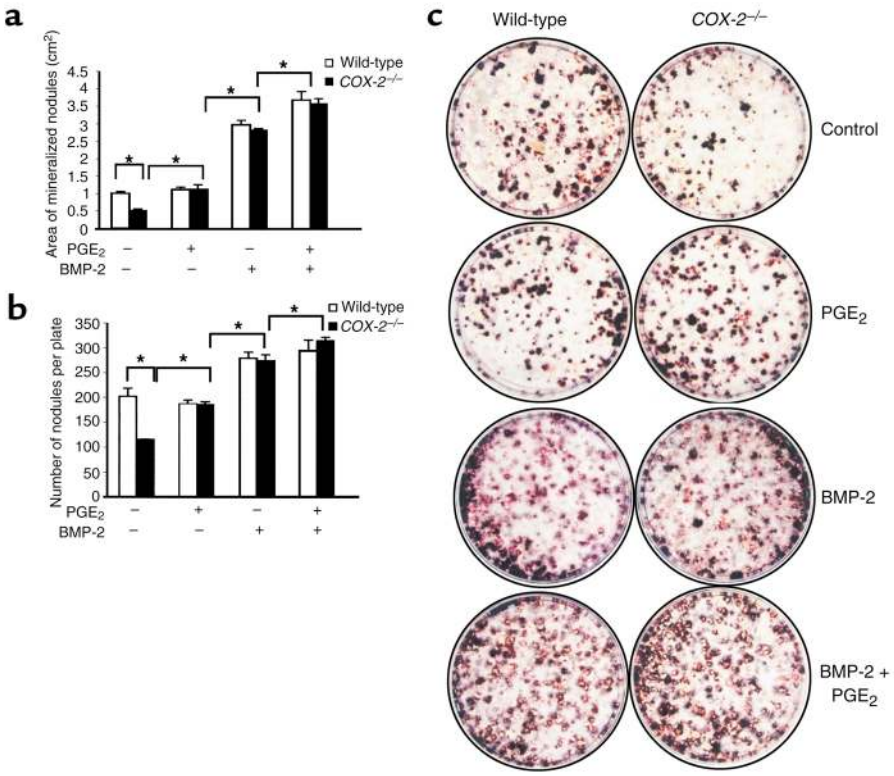

Figure 8
Defective bone marrow cell osteoblastogenesis can be compensated for by exogenous PGE_2 and BMP-2 in vitro. Bone marrow cells from four *COX-2*$^{-/-}$ mice and four littermate-controlled wild-type mice were pooled and cultured for 21 days in the presence of 50 μM L-ascorbic acid and 10 mM β-glycerophosphate. PGE_2 at 10^{-7} M was added on day 0, and 200 ng/ml BMP-2 was added on day 5. Von Kossa staining was used to examine bone nodule formation on day 21; representative photographs are shown (**c**). Nodule formation was quantified by counting the number of nodules per plate (**b**), and by determining the nodule area (**a**) using NIH image software in triplicate. Statistical significance compared with wild-type is indicated (*$P < 0.05$).

with cultures containing BMP-2 alone, suggesting that cyclooxygenases are necessary for maximal osteogenesis in the presence of BMP signaling events.

COX-2 regulates cbfa1 and osterix expression during osteoblastogenesis. Recent studies have demonstrated that the transcription factors cbfa1 and osterix play essential roles in mesenchymal stem cell differentiation into osteoblasts (13–15), and furthermore, cbfa1 appears to act upstream of osterix (15). Since the phenotype of defective fracture healing in *COX-2*$^{-/-}$ mice mimics the developmental phenotype of the *cbfa1*$^{-/-}$ and *osterix*$^{-/-}$ mice, where an absence of mesenchymal cell osteoblastogenesis is observed, we investigated the expression of these genes in our cultures (Figure 9). Using quantitative real-time PCR, we found that *cbfa1* and *osterix* were significantly reduced in *COX-2*$^{-/-}$ cells (Figure 9). Consistent with the bone nodule data, *cbfa1* and *osterix* expression recovered to control levels with PGE2 treatment and were further enhanced by treatment with BMP-2. Furthermore, these factors in combination induced maximal expression of these genes. These data establish a mechanism by which COX-2 is required for the appropriate expression of two BMP-regulated genes, *cbfa1* and *osterix*, which are critical for normal bone formation during reparative events.

Discussion

Immediately following skeletal injury, a sequence of biochemical and cellular events commence to induce an inflammatory response. A myriad of factors including

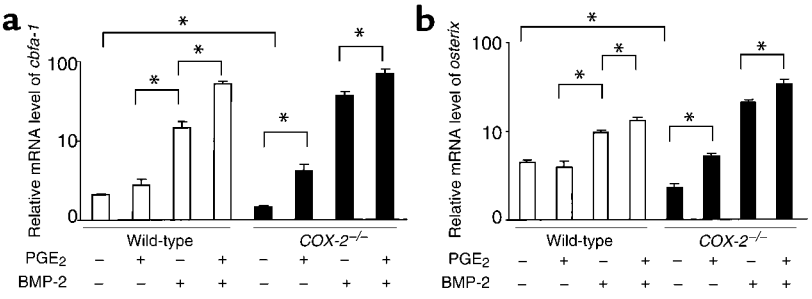

Figure 9
COX-2 regulates *cbfa1* and *osterix* in bone marrow stromal cell cultures. Bone marrow stromal cells from four wild-type or *COX-2*$^{-/-}$ mice were pooled and cultured as described previously. Total RNA was extracted on day 13 and real-time PCR was performed as described in the Methods. The relative expression of *cbfa1* (**a**) and *osterix* (**b**) mRNA, standardized to *actin*, was determined as described in Methods and is presented as the mean ± SEM in log scale. Statistical significance compared with wild-type is indicated (*$P < 0.05$).

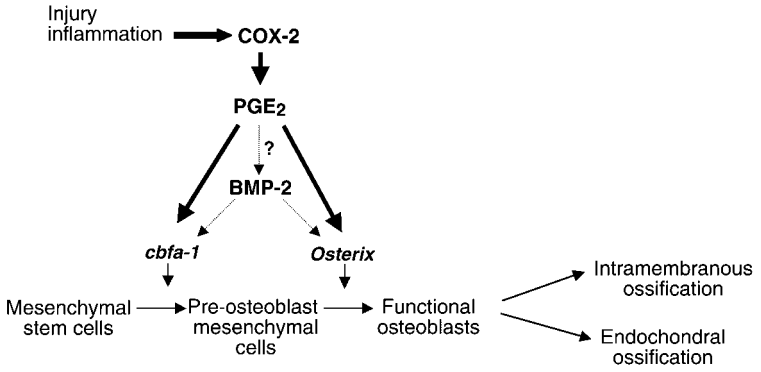

Figure 10
Schematic model representing the potential mechanism of COX-2 regulation of mesenchymal cell differentiation in bone repair. In the proposed model, COX-2 is induced in the early phase of the bone reparative process and produces increased amounts of PGE_2 in the local milieu. PGE_2 may induce BMPs and/or cooperate with BMPs to increase *cbfa1* and *osterix*, two essential transcription factors required for both endochondral and intramembranous bone formation.

growth factors, cytokines, and prostaglandins are released. These factors are likely to play an essential role initiating the healing response that leads to new bone formation (34). The crucial events in adult bone formation are the recruitment, proliferation, and differentiation of mesenchymal stem cells with endochondral and intramembranous bone formation at the injury site (35). In endochondral ossification, mesenchymal cells first differentiate into chondrocytes, which subsequently undergo terminal differentiation and apoptosis, leading to calcification of the matrix. The calcified matrix then serves as a template for primary bone formation, whereby osteoblasts deposit bone directly onto calcified cartilage (36). In intramembranous bone formation, mesenchymal cells differentiate directly into osteoblasts (36). Thus, both endochondral and intramembranous bone formation are dependent upon osteoblast differentiation from mesenchymal stem cells. Although the mechanism of recruitment and stimulation of mesenchymal stem cell differentiation during adult bone regeneration is largely unknown, there is evidence suggesting that local inflammation plays an important role in the process (34).

Prostaglandin production and *COX-2* mRNA are increased in fracture callus during the first 2 weeks following injury (16, 37), suggesting a role in the early phase of bone healing. In this study we demonstrated that COX-2 knockout mice had persistence of mesenchymal cells at the fracture site as well as a significant delay of ossification of cartilage tissue. Most remarkable was the reduction in osteoblastogenesis, a finding that was confirmed by two independent in vivo models of intramembranous bone formation as well as by in vitro studies that demonstrated a critical requirement for COX-2 in osteoblastogenesis. These findings demonstrate that the production of COX-2 metabolites during the inflammatory phase is required for efficient bone healing and that mesenchymal cell differentiation is a major target of cyclooxygenase activity.

A more subtle phenotype was the persistence of uncalcified cartilage at the fracture site in *COX-2*$^{-/-}$ mice. By evaluating the expression of the established markers of chondrocyte terminal differentiation (*colX* and *MMP13*) (38, 39), we were able to show that this process still occurs in the absence of COX-2 (Figure 5 and data not shown), but primary bone formation on the cartilagenous template was absent. However, these experiments do not eliminate the possibility of an important effect of COX-2 on chondrocytes during endochondral bone formation in fracture repair. Similarly, the reduced number of osteoclasts in the fracture callus of *COX-2*$^{-/-}$ mice suggests a role for prostaglandins in fracture remodeling as suggested by previous studies (4, 5), but this is a relatively late event in fracture healing that requires additional investigation.

The use of two separate in vivo models of intramembranous bone formation demonstrates that COX-2 plays a role in osteoblast differentiation and bone formation in response to diverse stimuli. In the titanium implantation model, there is an initial period of inflammatory bone resorption, followed by the deposition of new bone. In the second model, recombinant FGF-1 was injected onto mouse calvaria. FGF-1 has been shown to stimulate cellular proliferation, differentiation, and chemotaxis during bone repair (40, 41), and local and systemic injections have been shown to increase bone formation in both calvaria and long bones (32). COX-2 was demonstrated to have an important role in bone formation in both of these models, suggesting that it has general importance for reparative events in bone.

Prior work has demonstrated that prostaglandins such as PGE_2 induce bone nodules to form in bone marrow stromal cell cultures (6, 42) and in cultured rat calvaria osteoblasts (43–46). Furthermore, systemic or local injection of PGE_2 stimulates bone formation in vivo and appears to induce osteoblastogenesis from bone marrow precursors (7, 47). Ex vivo cultures of bone marrow stromal cells from rats injected with PGE_2 for 2 weeks yield four times more mineralized bone nodules compared with cultures from vehicle-injected rats (47). Finally, Scutt et al. demonstrated that PGE_2 increases bone nodule formation in low-density cultures of rat bone marrow cells by recruiting osteoblast precursors from a population of nonadherent mesenchymal precursor cells present in the bone marrow (48). Our work, using a genetic model based upon marrow cell cultures obtained from *COX-1*$^{-/-}$ and *COX-2*$^{-/-}$ mice and wild-type littermates, confirms the prior findings and additionally implicates COX-2 as

the critical isoform involved in this process. Altogether, the studies suggest that prostaglandins play a role in osteoblast recruitment and differentiation.

The finding that the COX-2 metabolite PGE_2 can reverse the decrease in osteoblastogenesis observed in *COX-2*$^{-/-}$ marrow cell culture is not surprising given the effect of PGE_2 on bone formation both in vitro and in vivo (6, 7, 42, 47, 48). However, the finding that BMP-2 complements the deficiency in COX-2 and enhances bone nodule formation to a degree similar to that observed in wild-type cultures is particularly interesting and suggest that BMP signaling events may be downstream of COX-2 activity and PGE_2 effects. Furthermore, since induction of osteoblastogenesis by BMP-2, including bone nodule formation and *cbfa-1* and *osterix* expression, was further enhanced by PGE_2, it appears that BMPs and PGE_2 may also have independent and complementary effects. The latter observations are consistent with prior data demonstrating that PGE_2 enhances BMP-2–mediated osteoblast differentiation in human periodontal ligament cells (49).

Based on these findings, we propose a mechanism of action for COX-2 in bone repair (Figure 10). Under basal conditions, COX-2 activity maintains a population of mesenchymal stem cells in a pre-osteoblast state responsive to additional osteoblastic signals. During injury, elevated COX-2 expression increases the osteoblastic potential of mesenchymal stem cells and supports their differentiation to osteoblasts in response to osteogenic signals. COX-2 may exert its effect through regulation of the transcription factors cbfa1 and osterix. Since *cbfa-1* is upstream of *osterix*, the COX-2–dependent regulation is likely at this earlier stage of differentiation, although the findings do not rule out a direct effect of cyclooxygenase metabolites on *osterix* expression. Similarly, our findings showing BMP-2 complementation of COX-2 in vitro support the possibility that BMP signaling events could be downstream of cyclooxygenase metabolites, consistent with the recent demonstration of BMP-7 induction by PGE_2 in the osteoblast cell line U2-OS (50). However, the additive effects of PGE_2 and BMP-2 on osteoblastogenesis in our experiments also provide evidence for an independent role of these factors. This model postulates a unique mechanism of COX-2 in bone repair that is significantly different from that in fetal skeletal development. This mechanism may be particularly important in injury or during inflammation where large amounts of PGE_2 are produced by COX-2, as opposed to normal skeletogenesis where the role of COX-2 is limited.

In summary, we demonstrate that reparative bone formation is deficient in *COX-2*$^{-/-}$ mice and demonstrate a primary defect in osteoblastogenesis. The effect is associated with a decreased expression of two genes essential for osteoblastogenesis, *cbfa1* and *osterix*. Both intramembranous and endochondral bone formation are affected by the absence of COX-2. We further demonstrate that this defect is associated with abnormal mesenchymal cell recruitment and differentiation into osteoblasts. Our study raises concerns regarding the use of COX-2 inhibitors in patients who suffer from bone fractures or who are undergoing other types of bone repair.

Acknowledgments

This work was supported by research grants from the Orthopedic Research Education Foundation, the Musculoskeletal Transplant Foundation, and the NIH (AR-45971 and AR-46545). The authors thank F. Abuzzahab, M. Ulrich-Vinther, L.M. Flick, and P. Tiyapatanaputi for scoring the x-rays; B.F. Boyce and L. Xing for helpful discussion of this work; and J. Harvey for her assistance with histological work.

1. Kawaguchi, H., et al. 1994. Regulation of the two prostaglandin G/H synthases by parathyroid hormone, interleukin-1, cortisol, and prostaglandin E2 in cultured neonatal mouse calvariae. *Endocrinology*. **135**:1157–1164.
2. Raisz, L.G. 1995. Physiologic and pathologic roles of prostaglandins and other eicosanoids in bone metabolism. *J. Nutr.* **125**:2024S–2027S.
3. Raisz, L.G. 1999. Prostaglandins and bone: physiology and pathophysiology. *Osteoarthritis Cartilage*. **7**:419–421.
4. Okada, Y., et al. 2000. Prostaglandin G/H synthase-2 is required for maximal formation of osteoclast-like cells in culture. *J. Clin. Invest.* **105**:823–832.
5. Zhang, X., et al. 2001. Evidence for a direct role of COX-2 in implant wear debris induced osteolysis. *J. Bone Miner. Res.* **16**:660–669.
6. Weinreb, M., Suponitzky, I., and Keila, S. 1997. Systemic administration of an anabolic dose of PGE_2 in young rats increases the osteogenic capacity of bone marrow. *Bone*. **20**:521–526.
7. Suponitzky, I., and Weinreb, M. 1998. Differential effects of systemic prostaglandin E2 on bone mass in rat long bones and calvariae. *J. Endocrinol.* **156**:51–57.
8. Forwood, M.R. 1996. Inducible cyclo-oxygenase (COX-2) mediates the induction of bone formation by mechanical loading in vivo. *J. Bone Miner. Res.* **11**:1688–1693.
9. Duncan, R.L., and Turner, C.H. 1995. Mechanotransduction and the functional response of bone to mechanical strain. *Calcif. Tissue Int.* **57**:344–358.
10. Morham, S.G., et al. 1995. Prostaglandin synthase 2 gene disruption causes severe renal pathology in the mouse. *Cell*. **83**:473–482.
11. Langenbach, R., et al. 1995. Prostaglandin synthase 1 gene disruption in mice reduces arachidonic acid-induced inflammation and indomethacin-induced gastric ulceration. *Cell*. **83**:483–492.
12. Okada, Y., et al. 2000. Effects of cyclooxygenase-2 gene disruption on osteoblastic function. *J. Bone Miner. Res.* **15**(Suppl.):217.
13. Ducy, P., Zhang, R., Geoffroy, V., Ridall, A.L., and Karsenty, G. 1997. Osf2/Cbfa1: a transcriptional activator of osteoblast differentiation. *Cell*. **89**:747–754.
14. Komori, T., et al. 1997. Targeted disruption of cbfa1 results in a complete lack of bone formation owing to maturational arrest of osteoblasts. *Cell*. **89**:755–764.
15. Nakashima, K., et al. 2002. The novel zinc finger-containing transcription factor osterix is required for osteoblast differentiation and bone formation. *Cell*. **108**:17–29.
16. Dekel, S., Lenthall, G., and Francis, M.J. 1981. Release of prostaglandins from bone and muscle after tibial fracture. An experimental study in rabbits. *J. Bone Joint Surg. Br.* **63**:185–189.
17. Altman, R.D., et al. 1995. Effect of nonsteroidal antiinflammatory drugs on fracture healing: a laboratory study in rats. *J. Orthop. Trauma*. **9**:392–400.
18. Ho, M.L., Chang, J.K., and Wang, G.J. 1998. Effects of ketorolac on bone repair: a radiographic study in modeled demineralized bone matrix grafted rabbits. *Pharmacology*. **57**:148–159.
19. Giannoudis, P.V., et al. 2000. Nonunion of the femoral diaphysis. The influence of reaming and non-steroidal anti-inflammatory drugs. *J. Bone Joint Surg. Br.* **82**:655–658.
20. Glassman, S.D., et al. 1998. The effect of postoperative nonsteroidal anti-inflammatory drug administration on spinal fusion. *Spine*. **23**:834–838.
21. Keller, J., Klamer, A., Bak, B., and Suder, P. 1993. Effect of local prostaglandin E2 on fracture callus in rabbits. *Acta. Orthop. Scand.* **64**:59–63.
22. Keller, J. 1996. Effects of indomethacin and local prostaglandin E2 on fracture healing in rabbits. *Dan. Med. Bull.* **43**:317–329.
23. Norrdin, R.W., and Shih, M.S. 1988. Systemic effects of prostaglandin E2 on vertebral trabecular remodeling in beagles used in a healing study. *Calcif. Tissue. Int.* **42**:363–368.
24. Einhorn, T.A. 1998. The cell and molecular biology of fracture healing. *Clin. Orthop.* **355**(Suppl.):7–21.

25. Barnes, G.L., Kostenuik, P.J., Gerstenfeld, L.C., and Einhorn, T.A. 1999. Growth factor regulation of fracture repair. *J. Bone Miner. Res.* **14**:1805–1815.
26. Zhang, X., Morham, S.G., Langenbach, R., and Young, D.A. 1999. Malignant transformation and antineoplastic actions of nonsteroidal antiinflammatory drugs (NSAIDs) on cyclooxygenase-null embryo fibroblasts. *J. Exp. Med.* **190**:451–459.
27. Le, A.X., Miclau, T., Hu, D., and Helms, J.A. 2001. Molecular aspects of healing in stabilized and non-stabilized fractures. *J. Orthop. Res.* **19**:78–84.
28. Ferguson, C.M., Miclau, T., Hu, D., Alpern, E., and Helms, J.A. 1998. Common molecular pathways in skeletal morphogenesis and repair. *Ann. NY Acad. Sci.* **857**:33–42.
29. Bonnarens, F., and Einhorn, T.A. 1984. Production of a standard closed fracture in laboratory animal bone. *J. Orthop. Res.* **2**:97–101.
30. Flick, L.M.H., Boyce, J.L., and Schwarz, E.M. 2001. Improved identification of fracture callus using alcian blue hematoxylin and orange G/Eoroin counterstain. *J. Histotech*. In press.
31. Boyce, B.F., Aufdemorte, T.B., Garrett, I.R., Yates, A.J., and Mundy, G.R. 1989. Effects of interleukin-1 on bone turnover in normal mice. *Endocrinology*. **125**:1142–1150.
32. Dunstan, C.R., et al. 1999. Systemic administration of acidic fibroblast growth factor (FGF-1) prevents bone loss and increases new bone formation in ovariectomized rats. *J. Bone Miner. Res.* **14**:953–959.
33. Schwarz, E.M., et al. 2000. A quantitative small animal surrogate to evaluate drug efficacy in preventing wear debris-induced osteolysis. *J. Ortho. Res.* **18**:849–855.
34. Probst, A., and Spiegel, H.U. 1997. Cellular mechanisms of bone repair. *J. Invest. Surg.* **10**:77–86.
35. Bruder, S.P., Fink, D.J., and Caplan, A.I. 1994. Mesenchymal stem cells in bone development, bone repair, and skeletal regeneration therapy. *J. Cell Biochem.* **56**:283–294.
36. de Crombrugghe, B., Lefebvre, V., and Nakashima, K. 2001. Regulatory mechanisms in the pathways of cartilage and bone formation. *Curr. Opin. Cell Biol.* **13**:721–727.
37. Gerstenfeld, L., et al. 2002. Differential inhibition of fracture healing by non-specific and cyclooxygenase-2 (COX-2) specific non-steroidal antiinflammatory drugs. *Trans. Orthop. Res. Soc.* **27**:0239. (Abstr.)
38. O'Keefe, R., Puzas, J., Loveys, L., Hicks, D., and Rosier, R. 1994. Analysis of type II and type X collagen synthesis in cultured growth plate chondrocytes by in situ hybridization: rapid induction of type X collagen in culture. *J. Bone Miner. Res.* **9**:1713–1722.
39. Wu, C., et al. 2002. Proteolysis involving matrix metalloproteinase 13 (collagenase-3) is required for chondrocyte differentiation that is associated with matrix mineralization. *J. Bone Miner. Res.* **17**:639–651.
40. Rodan, S.B., Wesolowski, G., Thomas, K., and Rodan, G.A. 1987. Growth stimulation of rat calvaria osteoblastic cells by acidic fibroblast growth factor. *Endocrinology*. **121**:1917–1923.
41. Kotev-Emeth, S., Savion, N., Pri-chen, S., and Pitaru, S. 2000. Effect of maturation on the osteogenic response of cultured stromal bone marrow cells to basic fibroblast growth factor. *Bone*. **27**:777–783.
42. Weinreb, M., Grosskopf, A., and Shir, N. 1999. The anabolic effect of PGE2 in rat bone marrow cultures is mediated via the EP4 receptor subtype. *Am. J. Physiol.* **276**:E376–E383.
43. Kaneki, H., et al. 1999. Prostaglandin E2 stimulates the formation of mineralized bone nodules by a cAMP-independent mechanism in the culture of adult rat calvarial osteoblasts. *J. Cell Biochem.* **73**:36–48.
44. Tang, L.Y., Kimmel, D.B., Jee, W.S., and Yee, J.A. 1996. Functional characterization of prostaglandin E2 inducible osteogenic colony forming units in cultures of cells isolated from the neonatal rat calvarium. *J. Cell Physiol.* **166**:76–83.
45. Nagata, T., et al. 1994. Effect of prostaglandin E2 on mineralization of bone nodules formed by fetal rat calvarial cells. *Calcif. Tissue Int.* **55**:451–457.
46. Flanagan, A.M., and Chambers, T.J. 1992. Stimulation of bone nodule formation in vitro by prostaglandins E1 and E2. *Endocrinology*. **130**:443–448.
47. Keila, S., Kelner, A. and Weinreb, M. 2001. Systemic prostaglandin E2 increases cancellous bone formation and mass in aging rats and stimulates their bone marrow osteogenic capacity in vivo and in vitro. *J. Endocrinol.* **168**:131–139.
48. Scutt, A., Zeschnigk, M., and Bertram, P. 1995. PGE_2 induces the transition from non-adherent to adherent bone marrow mesenchymal precursor cells via a cAMP/EP2-mediated mechanism. *Prostaglandins.* **49**:383–395.
49. Takiguchi, T., et al. 1999. Effect of prostaglandin E2 on recombinant human bone morphogenetic protein-2-stimulated osteoblastic differentiation in human periodontal ligament cells. *J. Periodontal Res.* **34**:431–436.
50. Paralkar, V.M., et al. 2002. Regulation of BMP-7 expression by retinoic acid and prostaglandin E(2). *J. Cell Physiol.* **190**:207–217.